Journal of Applied Polymer Science

Gas Permeability of Thin Dense Films from Polymer Blend of Thermoplastic Elastomer and Polyolefin

Masamoto Uenishi,[1†] Noriaki Fukushima,[1‡] Masashi Teramachi,[1†] Masahiko Mizuta,[1†] Jun Kamo[1††] Toshinori Tsuru[2]

[1]Corporate Research Laboratories, Mitsubishi Rayon Co., Ltd., Ohtake, Hiroshima, 739-0093, Japan

[2]Department of Chemical Engineering, Hiroshima University, Higashi-Hiroshima, Hiroshima, 739-8527, Japan

[†]Present address: Toyohashi Corporate Research Laboratories, Mitsubishi Rayon Co., Ltd., 4-1-2 Ushikawa-Dohri, Toyohashi, Aichi 440-8601, Japan.

[‡]Present address: Head Office, Mitsubishi Rayon Co., Ltd., 1-1, Marunouchi 1-Chome, Chiyoda-ku, Tokyo 100-8253, Japan.

[††]Present address: Graduate School of Engineering, Nagasaki University, 1-14 Bunkyo, Nagasaki 852-8521, Japan.

Correspondence to: M. Uenishi (E-mail: uenishi_ma@mrc.co.jp)

ABSTRACT: Stretched thin films composed of a thermoplastic elastomer, a polystyrene-*block*-poly(ethylene butylene)-*block*-polystyrene triblock copolymer (SEBS), and polyolefins, poly(ethylene-*co*-ethylacrylate) and poly(ethylene-*co*-propylene), were obtained by blow-molding, uniaxial stretching, and cooling to room temperature and the gas permeability of the stretched films was investigated. When the as-blown annealed film was subjected to uniaxial stretching in the machine direction, P_{O2} and P_{N2} increased with an increase in the stretching ratio K and approached a constant value at high stretching ratios. In addition, P_{O2}/P_{N2} decreased gradually with K and approached a value of 2.95–3.0. The reason for this unique gas permeation behavior is that the molecular mobility of poly(ethylene butylene) chains in a direction normal to the film increases and reaches an equilibrium state at around $K = 4.5$. The change in gas permeability of the stretched films can be explained using a deformation model for the SEBS matrix. © 2013 Wiley Periodicals, Inc. J. Appl. Polym. Sci. **2014**, *131*, 39386.

KEYWORDS: elastomers; polyolefins; membranes; blends; structure-property relations

Received 14 January 2013; accepted 4 April 2013

DOI: 10.1002/app.39386

INTRODUCTION

In the semiconductor manufacturing process, prevention of small defects is very important, because such defects lower the product yield rate. If small bubbles form in the liquid chemicals used [e.g., isopropyl alcohol, photoresist polymer solution, and developer solution] in the manufacturing process, this leads to the formation of defects.[1] To remove small bubbles in these liquid chemicals, a separation method using a thin dense, highly gas permeable membrane can be applied.[2]

To produce thin dense membranes, a melt extrusion and stretching process is preferable since a solvent evaporation method[3] tends to lead to contamination by residual solvent in the membrane. Thermoplastic polymer materials with high gas permeability, flexibility, and resistance to typical liquid chemical are preferable for use as degassing membrane materials. Thermoplastic elastomers and polyolefins are the candidate materials currently being considered for such membranes.[4]

Using a thermoplastic elastomer [e.g., polystyrene-*block*-poly(ethylene butylene)-*block*-polystyrene triblock copolymer (SEBS)], thin films can be produced by stretching at temperatures sufficiently higher than the glass transition temperature for the polystyrene domains. However, upon cooling to room temperature, physical crosslinking of the polystyrene domains reoccurs, leading to elastic recovery and a return to the original thickness.[5] For this reason, thin films of this thermoplastic elastomer are difficult to produce. In contrast, thin dense films of polyolefins can be obtained by a melt-extrusion and stretching process. However, the gas permeability of the stretched film becomes very low as the amount of stretching is increased because the crystallinity increases and the mobility of the amorphous chains decreases.[6,7]

We have previously reported[8] that a thin dense membrane can be obtained by appropriate control of the morphology of a polymer blend consisting of both a thermoplastic elastomer and a polyolefin. The concept behind this type of morphology control is shown in Figure 1. In this example, the morphology corresponds to that produced by blow-molding, uniaxial stretching, and cooling. The thermoplastic elastomer is assumed to be SEBS. As shown in Figure 1(a), the as-blown annealed

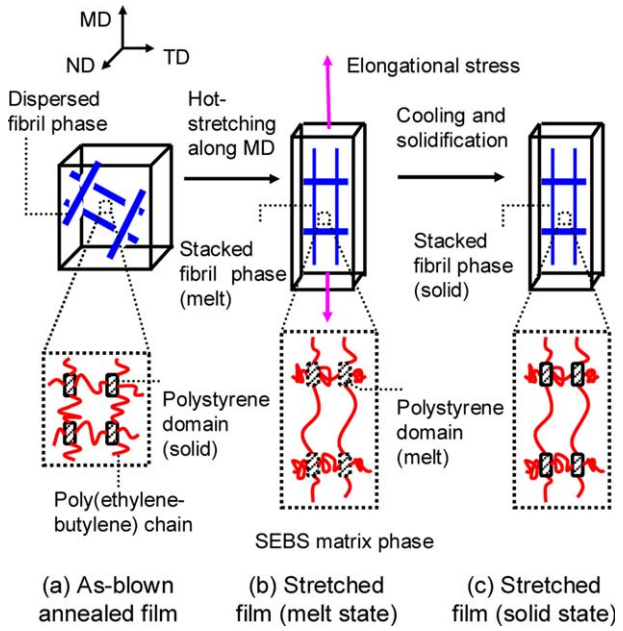

Figure 1. Concept of morphology control in a polymer blend film. [Color figure can be viewed in the online issue, which is available at wileyonlinelibrary.com.]

film consists of a dispersed fibril phase of polyolefin and a SEBS matrix phase. The SEBS matrix is also phase-separated into polystyrene domains and poly(ethylene-butylene) chains. The polystyrene domains act as crosslink points. Figure 1(b) shows the stretched film (melt state) under uniaxial hot stretching in the machine direction (MD). In this process, the crosslinking polystyrene domains melt, and the entire SEBS matrix phase becomes stretched. The dispersed fibril phase also melts and is stretched. As the stretching ratio increases, the thickness of the film decreases. In addition, the distance between neighboring fibrils decreases in the film thickness direction, and these fibrils eventually become stacked above each other. This stacked fibril phase forms a network-like structure that is co-continuous with the SEBS matrix. In Figure 1(c), when the stretched film is cooled to room temperature and solidifies, elastic recovery of the SEBS matrix is restricted by the stacked fibril phase so that the film remains thin.

In our previous article,[8] we also reported that a blow-molded film was prepared from the polymer blend material, MK-2F, that consisted of three constituents: SEBS (50 wt %) as a thermoplastic elastomer and poly(ethylene-*co*-ethylacrylate) (EEA; 30 wt %) and poly(ethylene-*co*-propylene) (EPP; 20 wt %) as polyolefin components. The as-blown annealed film was uniaxially stretched to confirm the morphology control concept. From morphological observations and viscoelastic measurements of the stretched films, the concept described above was realized.

In this study, blow-molded films prepared from MK-2F were uniaxially stretched and the relationship between the gas permeation behavior and the molecular mobility of the EB rubber chains during stretching was investigated. Unique gas permeation behavior was observed due to the fact that the molecular mobility of the poly(ethylene butylene) chains in the direction normal to the film increased and reached an equilibrium state at a stretching ratio of around 4.5.

Table I. Composition of MK-2F

	Composition (wt % of constituents)		
MK polymer	SEBS	EEA	EPP
MK-2F	50	30	20

Composition and structure were obtained by C^{13}-NMR and H^{1}-NMR analysis of an MK-2F pellet.

EXPERIMENTAL

Polymer Material

The composition, chemical structure, and thermal characteristics of each constituent in MK-2F are presented in Tables I, II, and III, respectively. From transmission electron microscopy (TEM) images[8] of the MK-2F pellet, it was determined that the polymer has a phase-separated structure with a SEBS matrix phase and a dispersed phase comprising a mixture of EEA and EPP with a fibril-like or droplet shape. The cylindrical polystyrene domains (diameter 200 Å) in the SEBS matrix were oriented along the MD, that is the extrusion direction of the MK polymer pellet and the spacing between the neighboring domains along the MD was very small, thereby forming a moniliform structure, as shown in Figure 2. Ethylene butylene chains (EB rubber chains or EB chains) existed in narrow regions (50–150 Å wide) between neighboring polystyrene domains.

Preparation of As-Blown Annealed Film

The as-blown film was prepared using the same melt-blowing process reported in the previous article.[8] The temperature of the melt-extrusion was 190°C. The polymer extrusion rate was 18 kg h^{-1} and the film was wound at a rate of 6.5 m min^{-1}. The blow ratio was MD/TD = 2/1. TD is transverse direction to the MD. The as-blown film (thickness 110 μm) had a cylindrical shape and was cut along the MD to obtain a rectangular film. This was then annealed for 16 h at 115°C (close to the T_g of the polystyrene domains) to achieve uniform orientation of the polystyrene domains in the SEBS matrix under tension-free conditions and subsequently cooled to room temperature; this is referred to as the as-blown annealed film.

Preparation of Stretched Films

Stretched films were produced by uniaxial stretching as shown in Figure 3. Both ends of an as-blown annealed film (110 × 85 mm^2, thickness 110 μm) were clamped with the clamp holder of a Tensilon Tester (Orientec RTC-1210A, Toyo Seiki Seisaku-sho, Japan) and subjected to uniaxial stretching in the MD at a hot stretching temperature of 70–160°C; the stretching area was 50 mm (MD) × 85 mm (TD) and the stretching rate was 20 mm min^{-1}. After the film was stretched, both ends were clamped by the clamp holder for 5 min. The film was cooled to room temperature (25°C) while still clamped and then removed from the clamp holder; this is referred to as the stretched film. The set value of the stretching ratio is given by $R = (MD_0 + \Delta R)/MD_0$, where ΔR is the movement distance from the initial

Table II. Chain Structure and Relative Fraction of Constituents in MK-2F

Constituent	Chain structure	Relative fraction (mol %)
SEBS	Polystyrene-*block*-poly(ethylene butylene)-*block*-polystyrene triblock copolymer	Styrene/(ethylene butylene) 7/93
		Ethylene/butylene 75/25
EEA	Ethylene-ethylacrylate random copolymer	Ethylene/ethylacrylate 96/4
EPP	Ethylene-propylene random copolymer	Ethylene/propylene 2/98
		Polypropylene tacticity:
		mm/mr/rr 95.9/2.7/1.4

Composition and structure were obtained by C^{13}-NMR and H^{1}-NMR analysis of an MK-2F pellet.

position of the cross-head in the Tensilon tester. The dimensional changes of the stretched films are expressed in terms of the stretching ratio K, film length ratio MD_1/MD_0, and film width ratio TD_1/TD_0. MD_0 and MD_1 are the lengths of the as-blown annealed film and the stretched film, respectively, and TD_0 and TD_1 are the widths of the as-blown annealed film and the stretched film, respectively. The stretching ratio K for uniaxial stretching is defined by eq. (1):

$$K = d_0/d_1 \tag{1}$$

where d_0 and d_1 are the thickness of the as-blown annealed film and the stretched film, respectively.

Characterization

Gas Permeability. Samples (55 mm diameter) were cut from the central portion of the as-blown annealed films and stretched films for measurement of the oxygen and nitrogen permeability coefficients using gas permeability measurement equipment (GTR-10H, GTR Tec, Kyoto, Japan) and gas chromatography (G2800, GTR Tec) at 25°C. For the gas chromatography data analysis, the Chromatopack CR3A (Shimadzu, Kyoto, Japan) was combined with the gas chromatography equipment. Pure oxygen and nitrogen were used for the gas permeability measurements. The feed pressure and permeate pressure were 113 cmHg and 0.07–0.1 mmHg, respectively. Sample films were 15.2 cm^2 in area.

The measurement errors of the gas permeability coefficient data for the as-blown annealed and stretched films were estimated using eqs. (2) and (3):

Table III. Thermal Properties of Constituents in MK-2F

Constituent	Glass transition	Melting	
	T_g (°C)	T_r (°C)	T_m (°C)
SEBS			
Poly(ethylene/butylenes)	-42	-50 to 32	16
Polystyrene	70		
EEA	-120	35 to 107	94
EPP	0	107 to 162	151

DSC measurement conditions: sample pellets were cooled to -150°C and then heated to 180°C at a heating rate of 10°C/min. T_g = glass transition temperature, T_r = temperature range from the start to the end of melting, T_m = melting point (DSC peak).

$$P_{O2} = P_{O2(m)} \pm \Delta\varepsilon_1 \tag{2}$$

$$P_{N2} = P_{N2(m)} \pm \Delta\varepsilon_2 \tag{3}$$

where P_{O2} and P_{N2} are true values of oxygen and nitrogen permeabilities, respectively, and $P_{O2(m)}$, $P_{N2(m)}$, $\Delta\varepsilon_1$, and $\Delta\varepsilon_2$ are measurement values of P_{O2} and P_{N2} and measurement errors in P_{O2} and P_{N2}, respectively.

The error $\Delta\varepsilon_3$ for P_{O2}/P_{N2} was estimated using eqs. (4) and (5).

$$\frac{P_{O2}}{P_{N2}} = \frac{P_{O2(m)}}{P_{N2(m)}} \pm \Delta\varepsilon_3 \tag{4}$$

$$\Delta\varepsilon_3 = \frac{P_{O2(m)}}{P_{N2(m)}}\left(\frac{\Delta\varepsilon_2}{P_{N2(m)}} + \frac{\Delta\varepsilon_1}{P_{O2(m)}}\right) \tag{5}$$

The values of $\Delta\varepsilon_1$, $\Delta\varepsilon_2$, and $\Delta\varepsilon_3$ for measurement data are represented by the error bars in Figures 7–9.

Five samples were used for the measurement of each sample film. Helium gas was used as the carrier gas in the gas chromatography.

Morphology. The morphologies of the as-blown annealed film and stretched films were observed using TEM (H-8000, Hitachi,

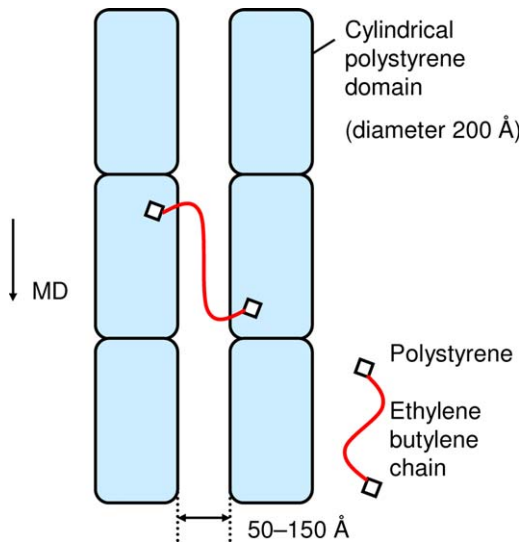

Figure 2. Polystyrene domains in the SEBS matrix in an MK-2F polymer pellet. Machine direction (MD): the extrusion direction of the MK polymer pellet. [Color figure can be viewed in the online issue, which is available at wileyonlinelibrary.com.]

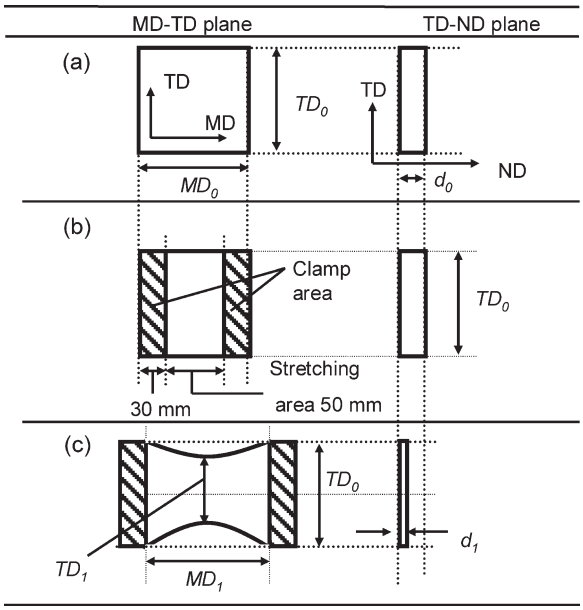

Figure 3. Preparation of uniaxially stretched film. (a) As-blown annealed film (MD_0 = 110 mm, TD_0 = 85 mm, d_0 = 0.11 mm), (b) set-up for stretching with clamped area indicated by cross-hatching, (c) stretched film, for example, MD_1 = 205 mm, d_1 = 0.025 mm, and TD_1 = 70 mm at a stretching temperature of 120°C, K = 4.1.

Japan, accelerating voltage 200 kV) with ultrathin sections stained with RuO_4. Sample sections (1–2 mm^2, 10 μm thick) were cut from a block of the sample and exposed to RuO_4 vapor generated from a RuO_4-water solution (0.5 wt % solution) at 40°C for 15 min. The exposed section was embedded in Spurr's epoxy resin[9] and hardened for 1 day at 60°C. The embedded stained section was cooled with liquid nitrogen and ultrathin sections (~70 nm thick) were sliced using an ultramicrotome.

DSC Measurements of As-Blown Annealed Films and Stretched Films. Differential scanning calorimetry (DSC) data for the as-blown annealed film and the stretched films were obtained using a DSC-6200 instrument (SII Nanotechnology, Tokyo, Japan) in a flow of nitrogen as the carrier gas. All heating scans were carried out from 25 to 200°C at 10°C min^{-1} under a first-heating process. The weight of each sample film was 4–5 mg. The measurement error in heat flow was ±0.5 mJ mg^{-1} for each of the values shown in the data.

Viscoelastic Properties of the Sample Films. The storage modulus E', loss modulus E'', and tan δ ($= E''/E'$) were measured using a dynamic mechanical spectrometer (DMS-200, SII Nanotechnology, Japan) using the tensile mode along the MD. Both ends of the film were clamped with the clamp holder of the measurement system. The film was heated from −150 to 150°C at a rate of 2°C min^{-1} and the viscoelastic properties were measured. Other measurement parameters were as follows: frequency, 10 Hz; mode, stretching deformation; sample film size in set-up, 10 mm (length) × 8 mm (width), in which the length direction was MD and the width direction TD. In general, in the linear viscoelastic region, strains are within 1% of the initial sample length.[10] In this experiment, the strain amplitude was set at ±0.5% of the initial sample length. The number of specimens evaluated for each sample was five in the viscoelastic measurements. The measurement accuracy was ±5% for each E', E'' data.

RESULTS AND DISCUSSION

Dimensional Changes of Stretched Films

Figure 4(a) shows the stretching ratio K, film length ratio MD_1/MD_0, and film width ratio TD_1/TD_0 after cooling at a stretching temperature of 70–140°C for a set-up value of stretching ratio of R = 4.0. After stretching at 70–80°C, recovery occurred once the sample film was removed from the clamp holders. K and MD_1/MD_0 of the recovered films were less than the initial set-up value of R = 4.0. In contrast, when stretching was performed at 90, 100, 120, and 140°C, the sample did not recover and K = 4 could be achieved. Figure 4(b) shows the stretching ratio K, film length ratio MD_1/MD_0, and film width ratio TD_1/TD_0 after cooling at stretching temperatures of 120 and 140°C

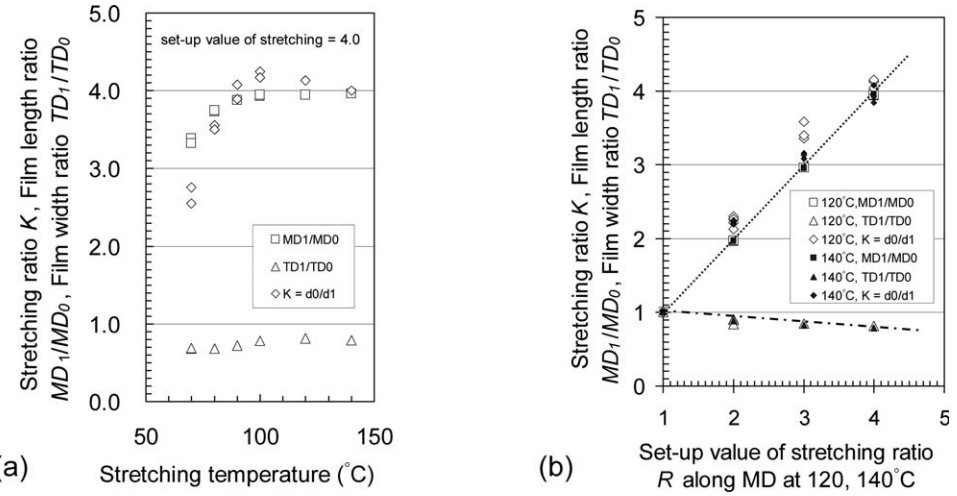

Figure 4. Dimensional changes of the stretched films. (a) Set-up value of stretching ratio = 4.0, stretching temperature = 70–140°C. (b) Set-up value of stretching ratio = 2.0–4.0, stretching temperature = 120, 140°C. MD_0 and MD_1 are the lengths of the as-blown annealed film and the stretched film, respectively. TD_0 and TD_1 are the widths of the as-blown annealed film and the stretched film, respectively. The lines in (b) represent data trends.

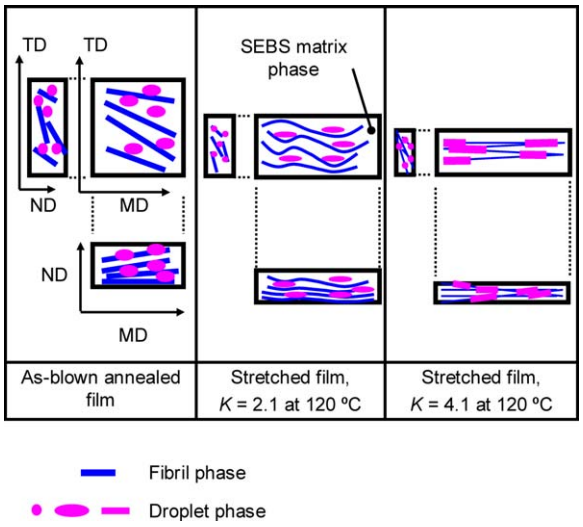

Figure 5. Morphology changes in the dispersed phase during uniaxial stretching and for the 3D-network formation mechanism. [Color figure can be viewed in the online issue, which is available at wileyonlinelibrary.com.]

for R = 2–4. Under these temperatures, K and MD_1/MD_0 increased linearly with R and the samples did not recover.

From Table III, at a stretching temperature of 70–80°C, polystyrene domains were just in the glass transition state and were not in a melt-flow state. Therefore, the SEBS matrix was not in a melt state. Also, the polyolefin (EEA and EPP) mixture phase was not fully melted. Therefore, the stretched film was recovered after release from the clamp. On the other hand, at a stretching temperature of 100–140°C, the physical crosslinking of the polystyrene domains was broken and the (EEA and EPP) mixture phase was partially melted. After cooling, a co-continuous structure [three-dimensional (3D)-network structure] of the SEBS phase and the (EEA+EPP) mixture phase was formed as mentioned in the Introduction section. Then, stretching recovery was not observed, as seen in Figure 4(b).

At high temperatures of 150–160°C, stretched films could not be obtained because the entire as-blown annealed film started to melt-flow and the shape of the film was not stable. The preferable stretching temperature was in the range of 100–140°C.

Restriction of Elastic Recovery

The key factors to restrict the elastic recovery for stretched film are as follows:

1. The formation of a 3D-network structure by the stacking between droplets and fibrils during hot stretching.
2. The uniform deformation of the entire film.
3. The solidification of the 3D-network while the both ends of the film were clamped.

In Figure 5, when the hot stretching was performed with an increase in the stretching ratio of K, the film thickness decreased and the fibrils were stacked with the droplets in a melted state. After the hot stretching, the 3D-network structure was immediately formed.[8]

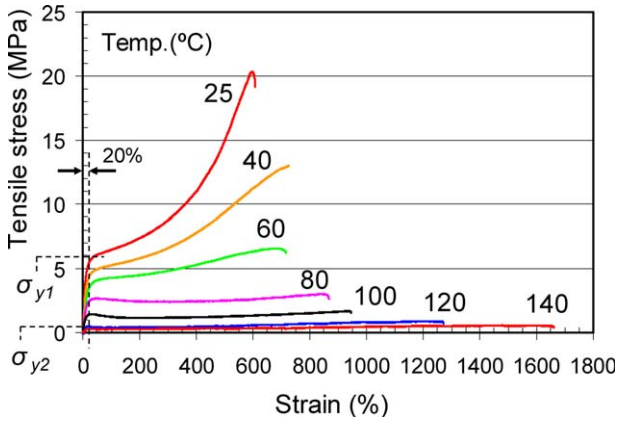

Figure 6. The stress–strain curves of the as-blown annealed film. Strain is defined as $\Delta MD/MD_0$, where ΔMD is the stretched length from MD_0 along the MD. The stretching rate was 20mm min^{-1}. [Color figure can be viewed in the online issue, which is available at wileyonlinelibrary.com.]

The stress–strain curves of the as-blown annealed film along MD[8] are shown in Figure 6. In the stretching curves at 100–140°C, the film was yielded at a strain of about 20% and then deformed as a viscous liquid at a strain of 20–1000%. The yield stress σ_{y2} at 120–140°C was smaller than that of σ_{y1} at 25°C. EEA and SEBS perfectly melt and EPP partially melts at 100–140°C (Table III).

In general, amorphous polymer chains entangle to form many physical crosslinks and the number of the entanglement differs for each polymer chain. If the polymer chains are stretched, the chains are subjected to the friction force from the entanglements and slip from the entanglements and are then deformed.[11] The degree of the friction force and also the degree of the deformation are not the same for each molecule. To obtain the uniform deformation for the molecules, it is necessary to maintain the stress for a time in order to obtain the equilibrium deformation for the molecules.

In our experiment, after the stretching, the film was clamped for 5 min before the film was cooled to room temperature. If the film is clamped for a short time (e.g., a few seconds) and cooled to room temperature, the equilibrium deformation of the EB rubber chain would not be obtained. In this case, since the molecular mobility of the EB rubber chain would be different in the measurement positions of the film, the measurement error in gas permeability of the film would be large. So, the stretched film should be maintained for as long as possible under the clamp force. Our results in Figures 7–9 show that the error bars in P_{O2}, P_{N2}, and P_{O2}/P_{N2} were small enough to obtain the data trends. Kotaka et al.[12] report that relaxation time for the elongation deformation in an SEBS polymer is on the order of 10^0–10^2 s. Five minutes (300 s) is enough time to obtain an equilibrium state for the molecular deformation.

On the cooling process, the stretched film was cooled to room temperature under the clamp. First, an EPP component crystallized and second, the styrene domain became a glass transition at about 90°C and finally, the ethylene unit in the EEA

Table IV. Gas Permeability of As-blown Film and As-blown Annealed Film

	Thickness (μm)	P_{O2}[a]	P_{N2}[a]	P_{O2}/P_{N2}
As-blown film	112.1	8.7	2.5	3.4
As-blown annealed film	112.1	9.2	2.7	3.4

[a] Units: 10^{-10} cm^3 (25°C) cm cm^{-2} s^{-1}(cmHg)$^{-1}$.

component crystallized at a the temperature that ranged from about 100°C to room temperature. After the crystallization of the EEA, the solidification of the 3D network was completely finished. On the other hand, if the stretched film was cooled to the T_g of the styrene domain (90°C) and released from the clamp, the recovery force from SEBS would immediately act on the entire film, but the crystallization of the EEA component would be not completed until well after it is cools to room temperature. In this case, the entire film would be immediately shrunk to a stable state and then the crystallization of the EEA component would be finished. The stretching ratio would be reduced and the film would be recovered to some degree. Therefore, the restriction of the elastic recovery of the film is completely finished by the solidification of the 3D-network structure.

Gas Permeability

As-Blown Film and As-Blown Annealed Film. The oxygen permeability P_{O2}, the nitrogen permeability P_{N2}, and the permeability ratio P_{O2}/P_{N2} for the as-blown film and as-blown annealed film ($K = 1$) are shown in Table IV. No major differences were found between the two films, confirming that the annealing process had no effect on the gas permeation behavior of the films.

Stretched Film

P_{O2}, P_{N2}, and P_{O2}/P_{N2} for the films stretched at 70–90°C and at 100–140°C for a stretching ratio $K = 1.5$–4.6 are shown in Figure 7(a,b), respectively. Figure 8 shows the effect of annealing for the stretched films ($K = 2.1$ at 120°C and $K = 4.1$ at 140°C) under tension-free conditions for 16 h. All data in Figures 7 and 8 are summarized in Figure 9. In these figures, the stretching ratio was determined using eq. (1) and the experimental results were plotted according to this ratio.

In Figure 7(a), it is seen that after stretching at 70–80°C, recovery occurred and the actual stretching ratio K was less than its initial set-up value R. With an increase of the stretching ratio K, P_{O2} and P_{N2} of the stretched films each increased and the corresponding P_{O2}/P_{N2} values decreased.

In Figure 7(b), for the stretched film at temperatures of 100, 120, and 140°C, both P_{O2} and P_{N2} increased gradually with K, reached a maximum at around $K = 2.1$, and then reached a constant value at high stretching ratios ($K > 4$). P_{O2}/P_{N2} decreased from 3.4 ($K = 1$) to around 2.95 ($K = 3$–3.5) and reached a constant value of around 2.95 ($K > 4$).

As shown in Figure 8, after the annealing of the stretched film at 120°C ($K = 2.1$), the stretching ratio decreased to $K = 1.6$ and P_{O2}, P_{N2}, and P_{O2}/P_{N2} changed to the values in the direction of the solid-line arrows. The same trends were observed for annealing of the stretched film at 140°C ($K = 3.73$) as shown by the dashed-line arrows.

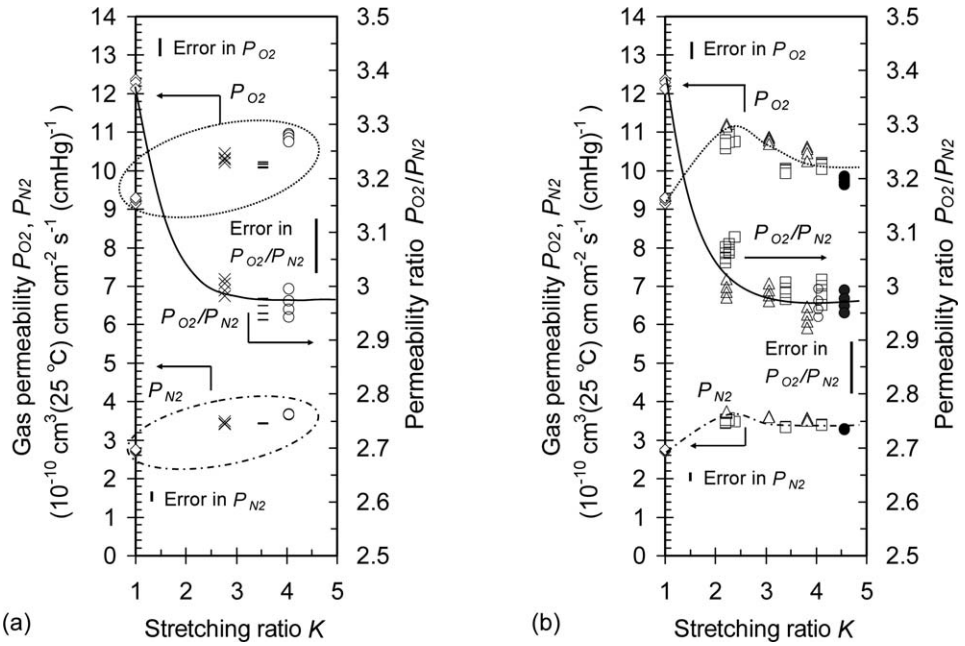

Figure 7. Gas permeability and permeability ratio for as-blown annealed film ($K = 1$) and stretched films. (a) As-blown annealed film ($K = 1$) and stretched films at stretching temperature of 70–90°C. (b) As-blown annealed film ($K = 1$) and stretched films at stretching temperature of 100–140°C. The lines on the graphs represent trend curves. Keys in (a), (b): as-blown annealed film (◇), stretched films 70°C (×), 80°C (–), 90°C (○), 100°C (•), 120°C (□), and 140°C (Δ).The stretching rate for all stretching processes was 20 mm min^{-1}.

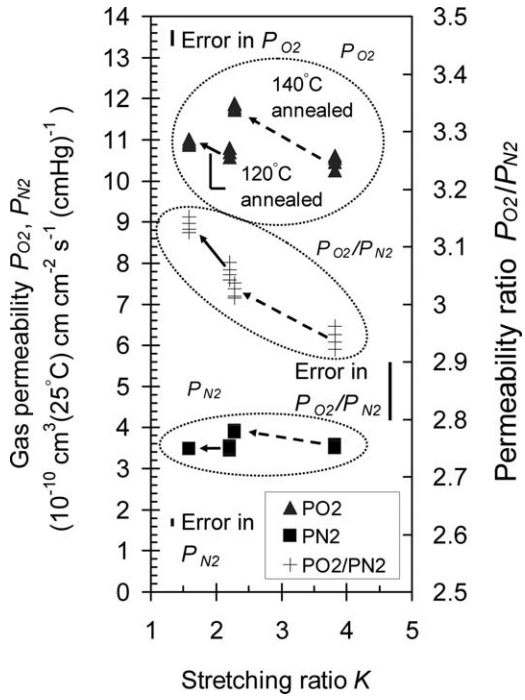

Figure 8. Gas permeability and permeability ratio after annealing. Keys: P_{O2} (▲), P_{N2}(■), P_{O2}/P_{N2}(+). The stretching rate for all stretching processes was 20 mm min^{-1}.

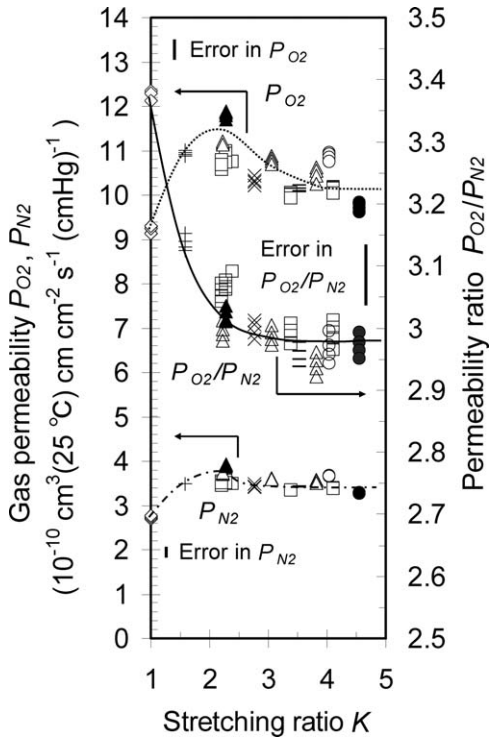

Figure 9. Gas permeability and permeability ratio (summary of results in Figures 5 and 6).

In Figure 9, each data of P_{O2}, P_{N2}, and P_{O2}/P_{N2} was found to lie on a master curve. These master curves showed that P_{O2} and P_{N2} initially increased with K and reached a maximum at about $K = 2.1$ before slightly decreasing and finally becoming constant at around $K = 4.5$. Moreover, P_{O2}/P_{N2} decreased with increasing K and became constant (~2.95–3.0) at around $K = 4.5$. Interestingly, regardless of whether recovery occurred or not, the gas permeability coefficient of the stretched films followed a master curve which depended on K. Moreover, even if the stretching temperature was different, P_{O2}, P_{N2}, and P_{O2}/P_{N2} could be expressed by a master curve as a function of K. The master curve lines for P_{O2}, P_{N2}, and P_{O2}/P_{N2} were significant data trends from the consideration of the measurement error bars.

In general, when an amorphous polymer material is stretched, the degree of orientation of the polymer chains increases, which results in lower molecular mobility for the chains. Therefore, the diffusion coefficient for gas molecules decreases, leading to a reduced gas permeability coefficient.[13–15] As reported by Wang and Porter,[15] when a compression-molded film of polystyrene [$P_{CO2} = 7.98 \times 10^{-10}$ cm^3 (STP) cm cm^{-2} s^{-1} (cmHg)$^{-1}$, where P_{CO2} is the gas permeability of carbon dioxide] was stretched to $K = 3.1$ and $K = 5.0$, its permeability was reduced to $P_{CO2} = 2.90 \times 10^{-10}$ cm^3 (STP) cm cm^{-2} s^{-1} (cmHg)$^{-1}$ and $P_{CO2} = 1.00 \times 10^{-10}$ cm^3 (STP) cm cm^{-2} s^{-1} (cmHg)$^{-1}$, respectively.

It has also been reported that if a semicrystalline polymer material is stretched, both the crystallinity and degree of crystal orientation increase, which leads to a decline in the diffusion coefficient of gas molecules and the gas permeability coefficient.[13–19] Holden et al.[16] reported that when a compression-molded film of high-density polyethylene ($P_{He} = 1.77 \times 10^{-10}$ cm^3 (STP) cm cm^{-2} s^{-1} (cmHg)$^{-1}$, where P_{He} is the helium gas permeability of the film) was stretched to $K = 10.0$ and $K = 20.5$, its permeability decreased to $P_{He} = 1.18 \times 10^{-10}$ cm^3 (STP) cm cm^{-2} s^{-1} (cmHg)$^{-1}$ and $P_{He} = 0.17 \times 10^{-10}$ cm^3 (STP) cm cm^{-2} s^{-1} (cmHg)$^{-1}$, respectively.

Hiltner et al.[20] reported that several compositions of poly(ether block amide) copolymer containing poly(tetramethylene oxide) and polyamide-12 exhibited a significant decrease in gas permeability upon uniaxial stretching. For Pebax 2533 grade (poly(tetramethylene oxide) 86 mol %, polyamide 14 mol %), both O_2 and CO_2 permeabilities decreased by 3.5 for the 400% stretched film ($K = 4.0$) compared to the unoriented film. This decrease in permeability was attributed to the crystallinity increase resulting from strain-induced crystallization of poly(tetramethylene oxide) soft blocks.

As summarized in Figure 9, when an as-blown annealed film was uniaxially stretched, P_{O2} and P_{N2} increased gradually with K and reached a constant value at around $K = 4.5$, irrespective of stretching conditions. P_{O2}/P_{N2} decreased with an increase in K and reached a constant value at around $K = 4.5$. This gas permeation behavior is indeed very interesting.

DSC Data for As-Blown Annealed Film and Stretched Films. Figure 10 shows DSC data for the as-blown annealed film and stretched films (120°C, K =2.1 and 140°C, $K = 4.1$). Endothermic melting peaks of crystalline ethylene units in EEA (EEA melt) and those of propylene units in EPP (EPP melt) were observed at 40–105°C and 105–160°C, respectively. Table V

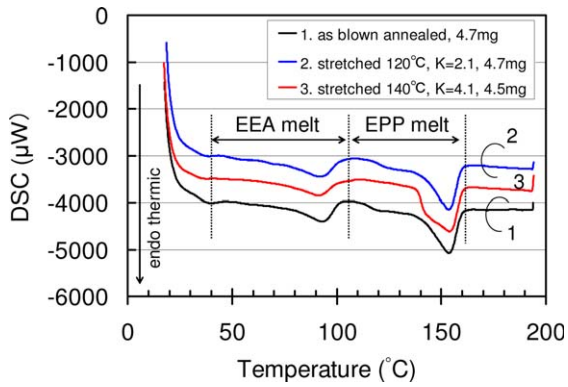

Figure 10. DSC traces of sample films. Data curves were scanned from 25 to 195°C in first heating at 10°C min^{-1}. 1; as-blown annealed film, 2; stretched film at 120°C, $K = 2.1$, 3; stretched film at 140°C, $K = 4.1$. [Color figure can be viewed in the online issue, which is available at wileyonlinelibrary.com.]

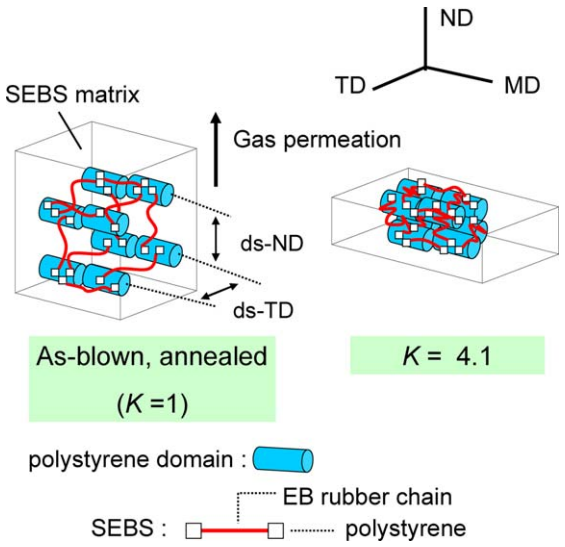

Figure 11. Deformation model for the SEBS matrix with gas permeation path. [Color figure can be viewed in the online issue, which is available at wileyonlinelibrary.com.]

shows that an increase in the heat of fusion (ΔH_f) that was in the range of the EPP melt for the stretched film (140°C, $K = 4.1$) compared with those for as-blown annealed film and stretched film at 120°C, $K = 2.1$. This might be due to stress-induced crystallization of EPP. The T_m melting peak position of EPP was not changed for the as-blown film and stretched films. Remarkable differences in endothermic heat flow for EEA and EPP were not observed between the as-blown annealed film and the stretched films ($K = 2.1$, 4.1). These results suggest that the crystallinity of EEA and EPP remained almost constant during stretching.

Gas Permeation Properties Based on the Deformation Model

Assumptions in the Model. The gas permeation path was added into the deformation model[8] that was originally proposed for the SEBS matrix, as shown in Figure 11. This model is based on the following four assumptions.

1. **Molecular mobility of EB rubber chain**: It has been reported[21,22] that the gas permeability coefficient of a polystyrene-*block*-polybutadiene-*block*-polystyrene triblock copolymer, which is a block copolymer similar to SEBS and in which polystyrene is the hard segment and polybutadiene is the soft segment, is mainly dependent on the molecular mobility of the butadiene rubber chains. Increasing the molecular mobility of the chains leads to an increase in the diffusion coefficient for gas molecules through the copolymer. Moreover, it has been reported that the gas permeability of other thermoplastic elastomers[23] and thermoplastic urethane polymers[24] are also mainly dependent on the molecular mobility of the soft segment. Based on the literature data,[21–24] it is assumed that the gas permeation behavior of the SEBS matrix is mainly dependent on the molecular mobility of the EB rubber chains.
2. **Gas permeability of the polyolefin components**: The oxygen permeabilities P_{O2} for EEA, PP, and SEBS are given in our previous report;[8] The P_{O2} values for EEA (8.2×10^{-10} cm^3 (STP) cm cm^{-2} s^{-1} $(cmHg)^{-1}$) and PP (2.3×10^{-10} cm^3 (STP) cm cm^{-2} s^{-1} $(cmHg)^{-1}$) are lower than that of SEBS (22.0×10^{-10} cm^3 (STP) cm cm^{-2} s^{-1} $(cmHg)^{-1}$). The value of P_{O2} for EPP is not clear, but it may be similar to that for PP. In the polyolefin components, if EEA and EPP are mixed uniformly in the MK polymer pellet (EEA 30 wt %, EPP 20 wt %), then P_{O2} for the dispersion phase becomes 2.9×10^{-10} cm^3 (STP) cm cm^{-2} s^{-1} $(cmHg)^{-1}$ by the additive rule, which is approximately one order of magnitude smaller than P_{O2} for SEBS. Therefore, in this deformation model, P_{O2} for the dispersion phase is considered to have a constant value of 2.9×10^{-10} cm^3 (STP) cm cm^{-2} s^{-1} $(cmHg)^{-1}$.
3. **Affine deformation of EB rubber chain**:[8] EB rubber chains have rubber-like elasticity and the Poisson ratio of the EB chain is 0.49.[25] Therefore, it is assumed that the EB rubber chains undergo affine deformation. The volume that the rubber chains occupy becomes invariant and the chains contract in both the ND and TD and extend in the MD during stretching.

Table V. Heat of Fusion (ΔH_f) for As-blown Annealed Film and Stretched Films

No.	Film	ΔH_f of EEA melt (mJ/mg)	ΔH_f of EPP melt (mJ/mg)
1	As-blown annealed	10.3	17.2
2	Stretched 120°C, $K = 2.1$	10.4	17.2
3	Stretched 140°C, $K = 4.1$	10.4	21.1

Table VI. Change in Spacing between Polystyrene Domains

Film	ds-ND (Å)	ds-TD(Å)
As-blown annealed	107-143	100-107
K = 2.1	67-100	67-100
K = 4.1	67-100	50-70

4. **No deformation of polystyrene domains:**[8] The Young's modulus for the polystyrene domains (24 MPa) is larger than that for EB chains (6.4 MPa);[25] therefore, it could be assumed that the polystyrene domain shape does not change during stretching.

From assumptions 1 and 2, the gas permeability coefficient of the entire film mainly depends on the mobility of the EB rubber chains of the SEBS matrix.

Gas Permeation Behavior Based on the Model. In our previous work,[8] we reported that the SEBS phase and polyolefin phase formed a bi-continuous structure in the stretched films and the gas molecules could pass through the SEBS matrix in the direction of the film thickness. Table VI shows the change in ds-ND and ds-TD, which are the spacings between polystyrene domains, during stretching. These values were measured from higher magnification TEM micrographs. Both ds-ND and ds-TD decreased up to K = 2.1, but became almost constant at K = 4.1. The assumption of affine deformation (assumption 3) suggests that if the EB rubber chains extend to the MD, they contract in both the TD and the ND. This affine deformation assumption is supported by data in Table VI. In the structural model shown in Figure 11, the

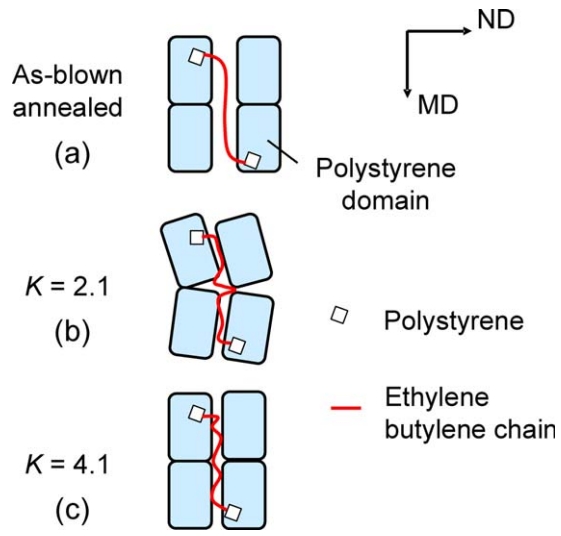

Figure 12. Undulation behavior of polystyrene domains in stretched SEBS matrix. [Color figure can be viewed in the online issue, which is available at wileyonlinelibrary.com.]

decrease in ds-ND and ds-TD indicates a relaxation of the EB rubber chains and an increase in their molecular mobility in the ND and TD. At a high stretching ratio (e.g., K = 4.1), the molecular mobility in the ND is expected to reach an equilibrium state. Therefore, the gas permeation behavior shown in Figures 7–9 could be explained by the increase in molecular mobility of the EB rubber chain in the ND. At high stretching ratios, the molecular mobility reached an equilibrium state.

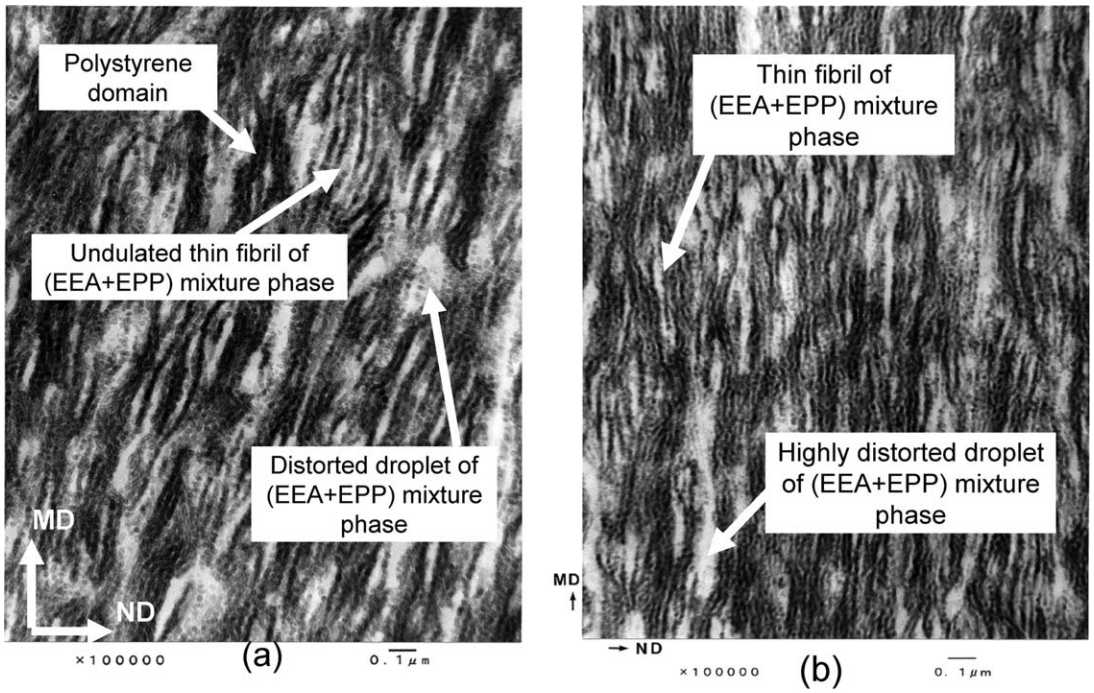

Figure 13. TEM micrographs of the stretched films in the MD-ND plane (K = 2.1, 4.1 at 120°C). (a) K = 2.1 and (b) K = 4.1. Bright regions represent the dispersed phase of the (EEA and EPP) mixture, while the dark regions correspond to the SEBS matrix phase. Polystyrene domains (cylindrical shape) in the SEBS matrix are stained dark with RuO_4 vapor.

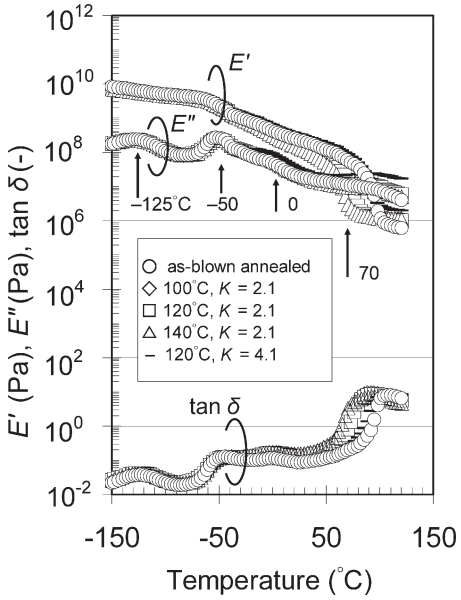

Figure 14. Viscoelastic properties of the as-blown annealed film and stretched films along MD. Keys: as-blown annealed (○), stretched at 100°C and $K = 2.1$ (◇), 120°C and $K = 2.1$ (□), 140°C and $K = 2.1$ (Δ), and 120°C and $K = 4.1$ (–). The arrow at –125°C corresponds to T_g of the ethylene units in EEA, other arrows at –50, 0, and 70°C correspond to T_g of the EB rubber chain in the SEBS, to T_g of the propylene units in EPP, and to T_g of the polystyrene units, respectively.

When the stretching ratio increased to around $K = 2.1$, P_{O2} and P_{N2} achieved their maximum values [Figures 7(b) and 9]. This was due to the increase in the molecular mobility of the EB rubber chains in the ND with undulation of the polystyrene domains for $K = 2.1$, as shown in Figure 12. TEM observations for $K = 2.1$ at 120°C [Figure 13(a)] indicated that the thin fibril of the (EEA+EPP) mixture phase was undulated along the MD. The polystyrene domains in the SEBS matrix phase were also undulated in a similar manner. This undulation behavior of the polystyrene domains is schematically represented in Figure 12(b). In Figure 13(a), it is seen that distorted droplets of the (EEA-EPP) mixture phase exist in the SEBS matrix. These droplets disturb the direction of stretching deformation for both the SEBS matrix and the thin fibril phase so that undulation occurred.

Also, from the viscoelastic measurement results along the MD in Figure 14, E' decreased strongly at temperatures from –50 to 70°C for the curves of 120°C, $K = 2.1$ and 140°C, $K = 2.1$. The glass transition temperature of the EB rubber chain was –42°C and that of polystyrene was 70°C, as seen from Table III, and the corresponding glass transition behavior appeared in the tan δ curve at –50°C and at around 70°C in Figure 14, respectively. The remarkable E' decrease from –50 to 70°C for the curves of 120°C, $K = 2.1$ and 140°C, $K = 2.1$ indicates that the stress applied to the EB rubber chain relaxed and its molecular mobility increased to a maximum at $K = 2.1$ along MD. This increase in molecular mobility of the EB rubber chain along MD also led to the increase in the molecular mobility along the ND as shown in Figure 12(b).

With further stretching ($K = 4.1$), the undulation and its contribution to molecular mobility disappeared [Figures 12(c) and 13(b)] and tan δ for 120°C, $K = 4.1$ overlapped with that of the as-blown annealed film (Figure 14).

If the gas permeation behavior in Figures 7–9 was due to pinhole defects introduced during stretching, P_{O2} and P_{N2} would increase with stretching and P_{O2}/P_{N2} would reach 0.94, corresponding to the Knudsen selectivity for O_2 and N_2 (Knudsen selectivity $= [M_w(N_2)/M_w(O_2)]^{1/2} = 0.94$, $M_w(N_2) = 28$ and $M_w(O_2) = 32$), where M_w is molecular weight. However, in this study, P_{O2}/P_{N2} approached 2.95–3.0, confirming that the gas permeation behavior is not due to pinhole defects.

In Figure 9, when the stretching ratio was increased to 4.5, P_{O2}/P_{N2} saturated at a value of 2.95–3.0, which was similar to P_{O2}/P_{N2} (2.8–2.9) for hydrogenated polybutadiene (EB chain) and SEBS (Kraton G1652), as shown in Table VII. The data in Table VII are reliable for polymer films in which the residual stress is released. We consider that the EB rubber chains were sufficiently relaxed in the ND at this high stretching ratio, so that the mobility of the chain reached a maximum state, resulting in an increase in the gas diffusion coefficient for both oxygen and nitrogen. Therefore, the gas permeation behavior described in Figure 9 could be explained by the increase in molecular mobility of the EB rubber chain in the ND and its mobility was saturated at $K > 4$.

The stretching ratio K is a parameter of the deformation model for SEBS as shown in Figure 9 and also is a parameter of the gas permeation behavior of the entire film.

Table VII. Gas Permeability for Typical Thermoplastic Elastomer Materials

Thermoplastic elastomer materials	Trade name	Gas permeability[a]			Ref.
		O_2	N_2	O_2/N_2	
SEBS	KRATON G1652[b]	22.0[c]	7.7[c]	2.9[c]	26, 27
Hydrogenated polybutadiene[d]		11.3	4.0	2.8	28

[a] Units 10^{-10} cm^3 (25°C) cm cm^{-2} s^{-1} $(cmHg)^{-1}$.

[b] Products of Kraton Polymers LLC.

[c] Film cast from polymer solution by authors.

[d] Ethylene butylene copolymer, crystallinity 29%.

CONCLUSIONS

In this study, stretched thin films composed of a thermoplastic elastomer and polyolefins were obtained by uniaxial stretching and cooling to room temperature. When the as-blown annealed film was subjected to uniaxial stretching in the MD, P_{O2} and P_{N2} each increased with increasing stretching ratio K and became constant at high stretching ratios. In addition, P_{O2}/P_{N2} decreased gradually with K and saturated at a value of 2.95–3.0. The reason for this unique gas permeation behavior is that molecular mobility of the poly(ethylene butylene) chains in the direction normal to the film increases and reaches an equilibrium state at around $K = 4.5$. This change in gas permeability of the stretched film can be explained using a deformation model for the SEBS.

ACKNOWLEDGMENTS

The authors express our deep gratitude to Drs. Jun Nakauchi, former Senior Research Fellow, Mitsubishi Rayon Co., Ltd. and Akira Hasegawa, former Fellow, Mitsubishi Rayon Co., Ltd., for their encouragement and involvement in discussions concerning data interpretation for this research article.

REFERENCES

1. Endoh, M. In Handoutai Process Kyouhon (in Japanese); SEMI Forum Japan Program Committee, Ed.; SEMI Forum Japan: Tokyo, Japan, **2007**; p 94.
2. Ohya, H.; Ariyoshi, T. *Nittou-Gihou (Japanese)* **1996**, *34*, 21.
3. Mulder, M. In Basic principles of Membrane Technology, 2nd ed.; Kluwer Academic: Netherlands, **1996**; p 71.
4. McCarthy, R. A. In Encyclopedia of Polymer Science and Engineering, Mark, H. F.; Bikales, N. M.; Overberger, C. G.; Menges, G.; Kroschwitz, J. I., Eds.; Wiley: New York, **1989**; Vol. *3*, p 421.
5. Gergen, W. P.; Lutz, R. G.; Davison, S. In Thermoplastic Elastomers, 2nd ed.; Holden, G.; Legge N. R.; Quirk, R. P.; Shroeder, H. E., Eds.; Hanser: Munich, **1996**; Chapter 11, p 297.
6. Ward, I. M.; Sweeney, J. S. An Introduction to the Mechanical Properties of Solid Polymers, 2nd ed.; Wiley: New York, **2004**.
7. Nielsen, L. E.; Landel, R. F. Mechanical Properties of Polymers and Composites, 2nd ed.; Marcel Dekker: New York, **1994**; Chapter 5, P 280.
8. Uenishi, M.; Fukushima, N.; Teramachi, M.; Mizuta, M.; Kamo, J.; Tsuru, T. *J. Appl. Polym. Sci.* **2013**, *128*, 2447.
9. Spurr, A. R. J. *Ultrastruct. Res.* **1969**, *26*, 31.
10. Ward, I. M.; Sweeney, J. S. An Introduction to the Mechanical Properties of Solid Polymers, 2nd ed.; John Wiley & Sons: New York, **2004**; Chapter 6, P 79.
11. Ward, I. M.; Sweeney, J. S. An Introduction to the Mechanical Properties of Solid Polymers, 2nd ed.; John Wiley & Sons: New York, **2004**; Chapter 6, P 95.
12. Kotaka, T.; Okamoto, M.; Kojima, A.; Kwon, Y. K.; Nojima, S. *Polymer* **2001**, *42*, 3223.
13. Delassus, P. Kirk-Othmer Encyclopedia of Chemical Technology, 4th ed.; Wiley: New York, **1992**; Vol. *3*, p 931.
14. Koros, W. J.; Hellums, M. W. In Encyclopedia of Polymer Science and Engineering, Mark, H. F.; Bikales, N. M.; Overberger, C. G.; Menges, G.; Kroschwitz, J. I., Eds.; Wiley: New York, **1989**; *Supplemental Volume*, p *724*.
15. Wang, L. H.; Porter, R. S. J. *Polym. Sci. Part B: Polym. Phys.* **1984**, *22*, 1645.
16. Holden, P. S.; Orchard, G. A. J.; Ward, I. M. J. *Polym. Sci. Part B: Polym. Phys.* **1985**, *23*, 709.
17. Webb, J. A.; Bower, D. I.; Ward, I. M.; Cardew, P. T. J. *Polym. Sci. Part B: Polym. Phys.* **1993**, *31*, 743.
18. Srinivas, S.; Brant, P.; Huang, Y.; Paul, D. R. *Polym. Eng. Sci.* **2003**, *43*, 831.
19. Chau, C. C.; Raspor, O. C. J. *Polym. Sci. Part B: Polym. Phys.* **1990**, *28*, 631.
20. Armstrong, S.; Freeman, B.; Hiltner, A.; Baer, E. *Polymer* **2012**, *53*, 1383.
21. Odani, H.; Taira, K.; Nemoto, N.; Kurata, M. *Denki-Kagaku (in Japanese)* **1976**, *44*, 311.
22. Ferdinand, A.; Springer, J. *Colloid Polym. Sci.* **1989**, *267*, 1057.
23. Fitch, M. W.; Koros, W. J.; Nolen, R. L.; Carnes, J. R. J. *Appl. Polym. Sci.* **1993**, *47*, 1033.
24. Cao, N.; Pegoraro, M.; Bianchi, F.; Di Landro, L.; Zanderighi, L. J. *Appl. Polym. Sci.* **1993**, *48*, 1831.
25. Motomatsu, M.; Muzutani, W.; Tokumoto, H. *Polymer* **1999**, *38*, 1779.
26. Technical Bulletin of Gas Permeability of KRATON Rubber; Shell Chemical Company: **1995**.
27. Roland, C. M. Polymer Data Handbook; Oxford University Press: New York, **1999**; p 161.
28. Michaels, A. S.; Bixler, H. J. J. *Polym. Sci.* **1961**, *50*, 413.